NORSAR

ROYAL NORWEGIAN COUNCIL FOR SCIENTIFIC AND INDUSTRIAL RESEARCH

Scientific Report No. 2-80/81

SEMIANNUAL TECHNICAL SUMMARY 1 October 1980—31 March 1981

By
Alf Kr. Nilsen (ed.)

Kjeller, June 1981

VI. SUMMARY OF TECHNICAL REPORTS/PAPERS PREPARED

VI.1 NORESS Data Analysis

Extensive analysis of noise and signal recordings from the new 12-sensor NORESS miniarray of Fig. VI.1.1 is continuing. The research on this subject comprises the following items:

i) Coherence, correlation and dynamic structure of noise as a function of frequency and sensor separation
ii) Signal correlation as a function of frequency and sensor separation
iii) Redundancy sampling in order to avoid excessive beamsteering losses
iv) Automated signal parameter extraction
v) Event location.

As regards point iv), some simplified algorithms for reading onset time and amplitude of first-arriving phases have been developed and implemented in the routine analysis of conventional NORSAR data and have so far worked very satisfactorily (see Chapter VI.4). The location capability of the NORESS array is deemed good as local events in general are within 30 km of agency announced epicenter locations, see Mykkeltveit and Ringdal (1981).

Results on noise coherence are shown in Fig. VI.1.2. It can be seen that noise coherence at frequencies around 2 Hz reaches the random level for a distance of about 0.6 km, while the same level is reached at 0.3 km for 4 Hz.

The dynamic structure of the noise is of importance for the design of miniarrays, and in this regard high resolution wave number spectral analyses have been undertaken on NORESS noise records. Some of the results obtained here are displayed in Fig. VI.1.3, and the following comments apply: At lower frequencies in the range 0.25 to 0.40 Hz the noise has a clearly propagational character with observed velocities typical of fundamental and higher mode Rayleigh wave phase velocities. In the frequency range 0.50 to 1.00 Hz the noise appears to be more unorganized with broad peaks which also show frequency instability, and there are sometimes large differences between conventional and high resolution wave number spectra. However, for higher frequencies, in the range 1.5-4.0 Hz, the wave number spectra become rather peaked and at velocities indicating P waves travelling in the mantle. These results are

somewhat unexpected on two accounts, namely: i) the noise correlation falls off rapidly with sensor separation (see Fig. VI.1.2) and ii) for teleseismic events mantle attenuation would efficiently remove the higher frequencies. As regards the first problem an explanation could be tied to the fact that noise coherency estimation is based on the so-called block averaging approach which means that a multitude of coherent wavelets but with widely different phase shifts would not give significant coherency, but on the other hand could appear 'coherent' in the frequency wave number analysis. In case of the second problem, it seems difficult not to accept that mantle attenuation removes the higher frequencies of teleseismic P wave efficiently. Then unless the results are some artefact of the processing method itself, some sort of instrumental noise prior to the digitation in the field could be an explanation. However, as instrumental noise, based on previous experience, is significantly lower than the seismic noise even at 4.0 Hz, we have not a satisfactory explanation at present of the observation presented in Fig. VI.1.3.

In the following we present results bearing on noise and signal correlation across the NORESS sensors. Fig. VI.1.4 shows the recording at the 12 NORESS channels of a local event about 140 km away (6 Nov 1980, 14.53.02.2 G.M.T., 59.54°N 10.68°E, local magnitude M_L=2.1), and the time segments marked for noise, P and Lg phases were subjected to correlation analysis. The data were resampled at 100 Hz to achieve more precise shifts in the beamforming. Also, the correlation studies were performed on filtered data, using 5 different filters defined as follows:

Filter 1:	0.8-2.8 Hz	Butterworth bandpass (3rd order)
Filter 2:	1.2-3.2 Hz	-"-
Filter 3:	1.6-4.0 Hz	-"-
Filter 4:	2.0-4.8 Hz	-"-
Filter 5:	2.4-4.8 Hz	-"-

Noise suppression results are given in Fig. VI.1.5. This figure is derived as follows: For each filter, the noise suppression is first computed for a beam that includes all 12 channels. Then one channel is removed from the beam so as to have optimum noise suppression for the beam constructed from the

remaining 11 channels. This process is continued by removing one channel at a time. Generally at each stage in this process this results in removing the one channel that has the minimal average distance to the others. We see that the number of sensors required for optimum noise suppression increases with increasing frequency, but also that the noise suppression generally deteriorates from putting more sensors into the central part of the array. The results in Fig. VI.1.5 represent averages over the three consecutive noise time windows in Fig. VI.1.4, and all correlations were computed with zero lags.

Average noise correlation as a function of sensor separation up to 1500 m is given in Fig. VI.1.6 for the five frequency bands. Averaging is performed over all inter-sensor distances that fall within segments of 100 m each. In addition, averaging is done over the three noise time windows of Fig. VI.1.4.

Signal correlations are given in Figs. VI.1.7 and VI.1.8 for the phases denoted P and Lg in Fig. VI.1.4. For each phase, two consecutive time windows were analyzed, the first one containing the main arrival. For each phase, time shifts were introduced corresponding to the phase velocity and azimuth value that gave the best signal gain. The same set of time shifts was retained for the coda window correlation analysis. Relatively high correlation values are found throughout the range of NORESS sensor separations for the phase onsets. Noteworthy is the higher degree of organization in the Lg coda relative to the P coda.

The NORESS data analysis now proceeds with a study of SNR gains as a function of array layout, utilizing the above results on noise and signal correlations.

S. Mykkeltveit
E.S. Husebye
H. Bungum
K. Åstebøl, Univ. of Oslo

Reference

Mykkeltveit, S. and F. Ringdal (1981): Phase identification and event location at regional distance using small-aperture array data, in: 'Identification of Seismic Sources - Earthquake or Underground Explosion', E.S. Husebye and S. Mykkeltveit (eds.), D. Reidel Publ. Co., in press.

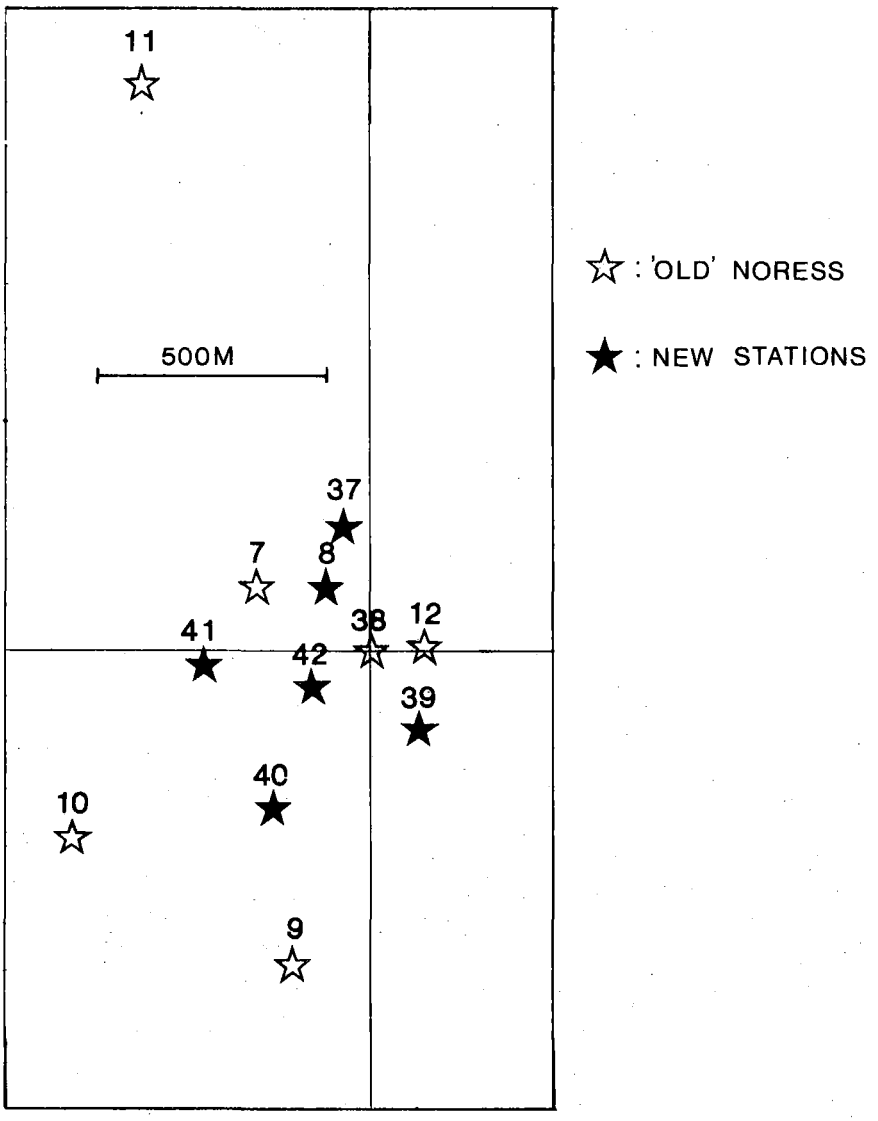

Fig. VI.1.1 Geometry of the new 12-channel NORESS array, which became operational on 28 October 1980.

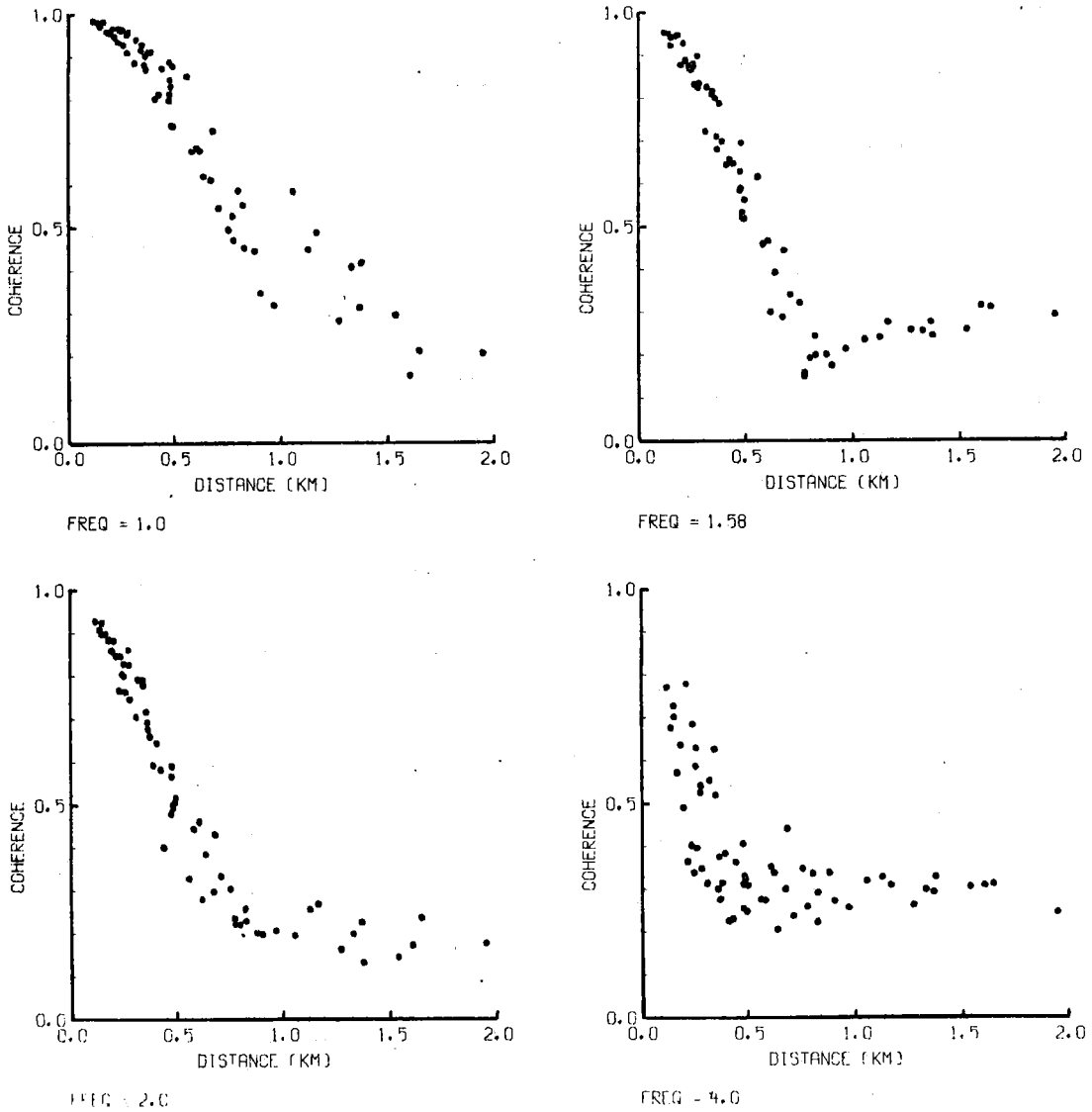

Fig. VI.1.2 NORESS noise coherence vs distance for a noise interval from day 310/80, for frequencies of 1.0, 1.5, 2.0 and 4.0 Hz. All combinations of the 12-channel array are used, and the estimates are based on averaging of 18 blocks each of 256 samples, with an additional smoothing around each of the analyzed frequencies.

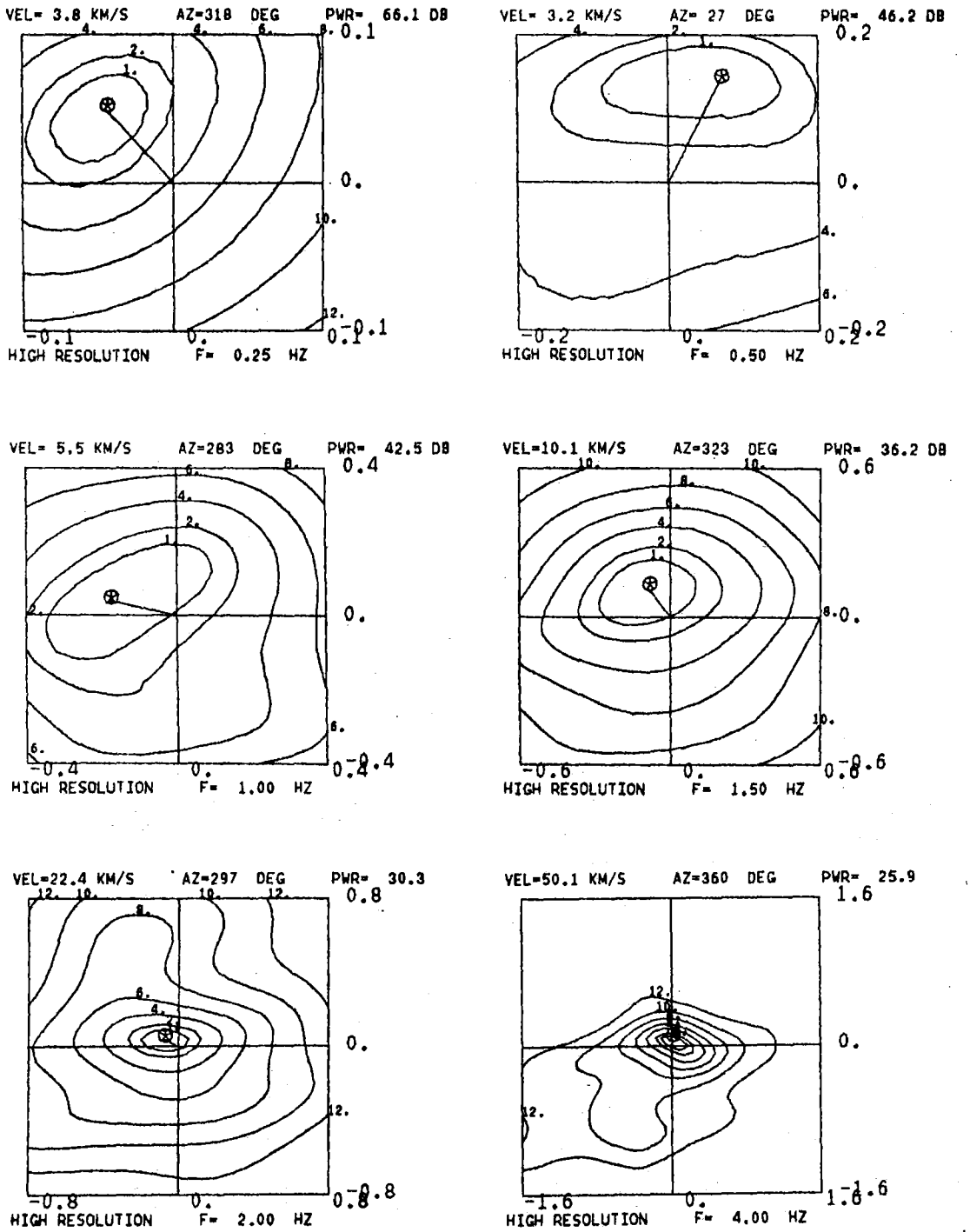

Fig. VI.1.3 High resolution wave number spectra for the data used in Fig. VI.1.2, and for the frequencies 0.25, 0.50, 1.0, 1.5, 2.0 and 4.0 Hz (the last four as in Fig. VI.1.2). The frames are scaled such that velocities down to 2.5 km/s are covered in each case, and the estimates are based on 16 blocks each of 250 samples of short period data sampled at 20 samples/sec.

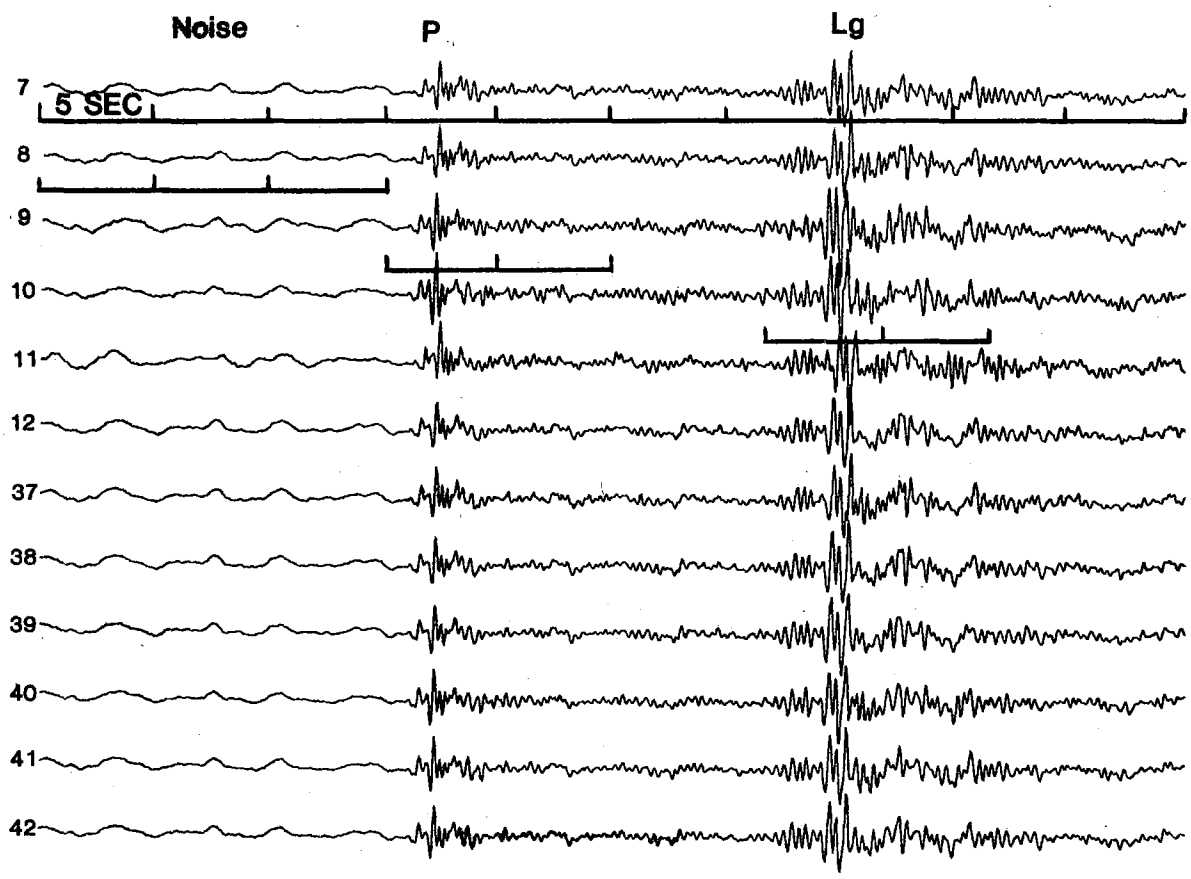

Fig. VI.1.4 Unfiltered data from the 12 NORESS stations. Channel numbers refer to Fig. VI.1.1. Epicentral distance is about 140 km. The marked time windows for noise, P and Lg phases were subjected to correlation analysis.

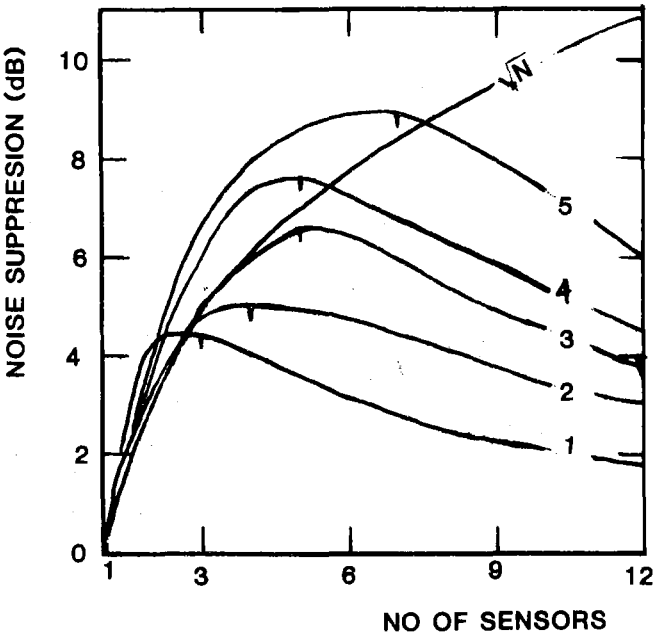

Fig. VI.1.5 Noise suppression for five different bandpass filters as a function of sensor number included in the beam (see text).

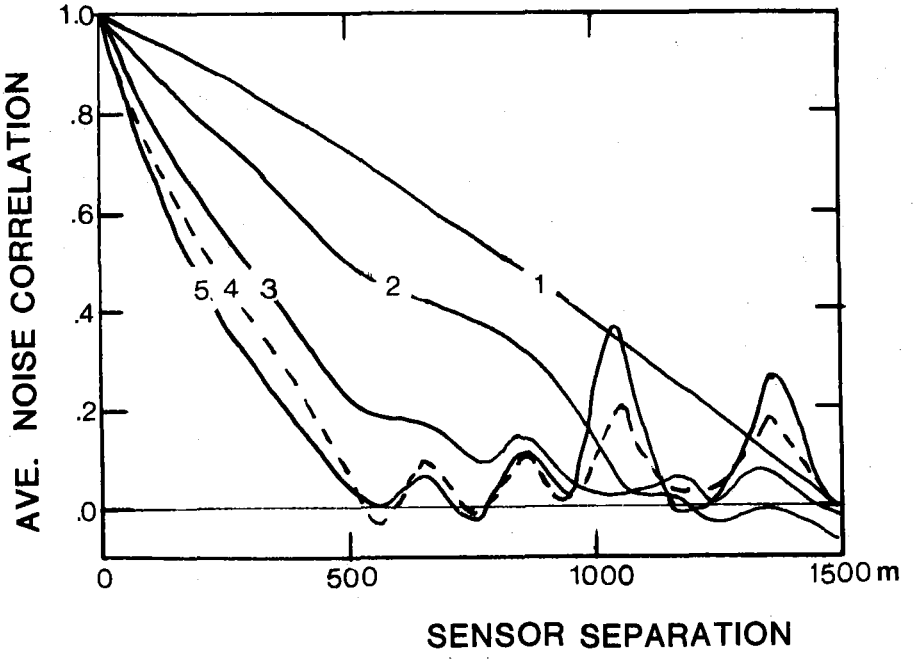

Fig. VI.1.6 Noise correlation as a function of sensor separation up to 1500 m. Averaging is performed over all sensor combinations that fall within segments of 100 m.

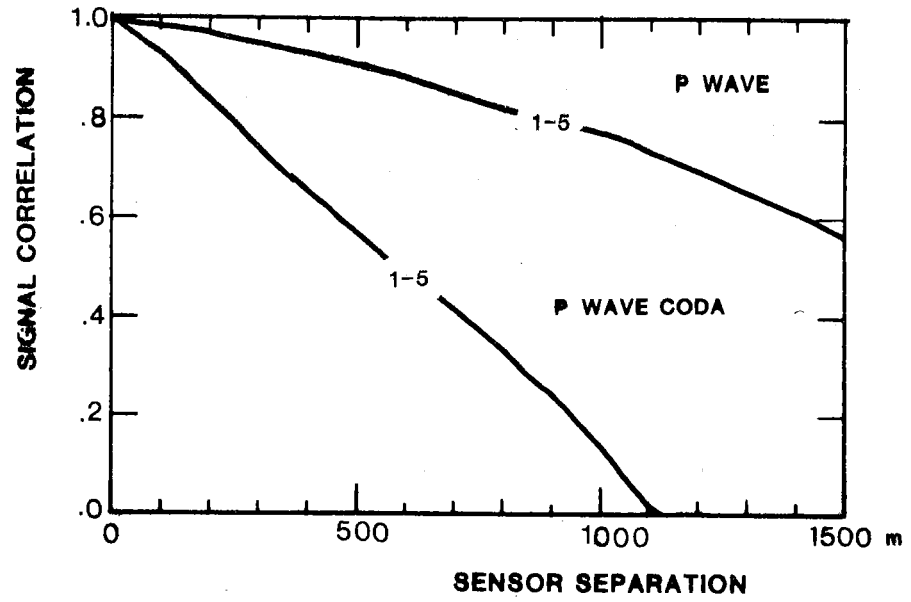

Fig. VI.1.7 P wave and P wave coda correlations as a function of sensor separation. The results are averaged over all five filters.

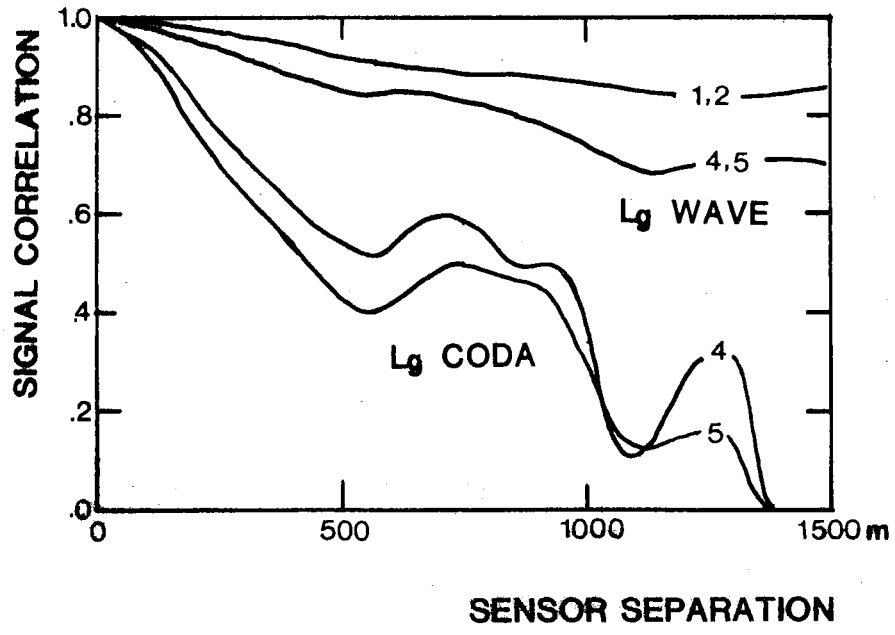

Fig. VI.1.8 Lg wave and Lg wave coda correlations as a function of sensor separation for the filters indicated.